

# Radiation Engineering of Optical Antennas for Maximum Field Enhancement

Tae Joon Seok,<sup>†,§</sup> Arash Jamshidi,<sup>†,§</sup> Myungki Kim,<sup>†</sup> Scott Dhuey,<sup>‡</sup> Amit Lakhani,<sup>†</sup> Hyuck Choo,<sup>†,‡</sup> Peter James Schuck,<sup>‡</sup> Stefano Cabrini,<sup>‡</sup> Adam M. Schwartzberg,<sup>‡</sup> Jeffrey Bokor,<sup>†,‡</sup> Eli Yablonovitch,<sup>†</sup> and Ming C. Wu<sup>\*,†</sup>

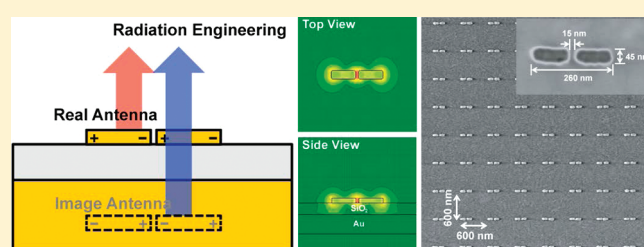
<sup>†</sup>Department of Electrical Engineering and Computer Sciences, University of California, Berkeley, California 94720, United States

<sup>‡</sup>Molecular Foundry, Lawrence Berkeley National Laboratory, Berkeley, California 94720, United States

**S** Supporting Information

**ABSTRACT:** Optical antennas have generated much interest in recent years due to their ability to focus optical energy beyond the diffraction limit, benefiting a broad range of applications such as sensitive photodetection, magnetic storage, and surface-enhanced Raman spectroscopy. To achieve the maximum field enhancement for an optical antenna, parameters such as the antenna dimensions, loading conditions, and coupling efficiency have been previously studied. Here, we present a framework, based on coupled-mode theory, to achieve maximum field enhancement in optical antennas through optimization of optical antennas' radiation characteristics. We demonstrate that the optimum condition is achieved when the radiation quality factor ( $Q_{\text{rad}}$ ) of optical antennas is matched to their absorption quality factor ( $Q_{\text{abs}}$ ). We achieve this condition experimentally by fabricating the optical antennas on a dielectric ( $\text{SiO}_2$ ) coated ground plane (metal substrate) and controlling the antenna radiation through optimizing the dielectric thickness. The dielectric thickness at which the matching condition occurs is approximately half of the quarter-wavelength thickness, typically used to achieve constructive interference, and leads to  $\sim 20\%$  higher field enhancement relative to a quarter-wavelength thick dielectric layer.

**KEYWORDS:** Plasmonics, nano-optics, optical antenna, ground plane, impedance matching



Optical antennas,<sup>1–3</sup> similar to their radio frequency (RF) counterparts, capture free-space electromagnetic radiation and focus it to a small region (such as the antenna feed gap) well beyond the diffraction limit. The amount of field enhancement in the high-field region of the optical antennas is the most important parameter used to characterize the performance of the antenna for applications such as sensitive photodetection,<sup>4</sup> heat-assisted magnetic recording,<sup>5</sup> and surface-enhanced Raman spectroscopy (SERS).<sup>6,7</sup> To maximize the field enhancement, careful optimization of optical antennas' characteristics<sup>14–16</sup> using antenna theory concepts needs to be explored. Tuning the resonance wavelength of optical antennas by changing the antenna dimensions,<sup>8</sup> loading the antenna gap with appropriate materials,<sup>9,10,14</sup> shrinking the size of antenna feed gap<sup>2</sup> to effectively reduce the mode volume, and using arrays of optical antennas<sup>11</sup> for improved coupling have been proposed and demonstrated to increase the amount of field enhancement.

In this paper, we present a new method, based on coupled mode theory (CMT),<sup>12,13</sup> to achieve maximum field enhancement in optical antennas through optimization of the antennas' radiation characteristics. Coupled mode theory has been used previously<sup>13</sup> to model the field enhancement of an optical antenna for applications such as SERS. In the CMT picture (Figure 1a), an optical antenna is modeled as a resonator and the excitation is modeled as an input channel. The field enhancement

of an optical antenna at resonance can be derived<sup>13</sup> (Supporting Information, Section I) as

$$\frac{|E_{\text{loc}}|^2}{|E_i|^2} = \frac{2A_c \lambda_{\text{res}}}{\pi} \frac{Q}{Q_{\text{rad}}} \frac{Q}{V_{\text{eff}}} \quad (1)$$

where  $E_{\text{loc}}$  and  $E_i$  are the local field amplitude at the high field region of an optical antenna and the field amplitude of incoming excitation beam, respectively,  $V_{\text{eff}}$  is the effective mode volume of the resonator, and  $A_c$  is the maximum effective aperture of the antenna that is determined by spatial mode matching between the antenna radiation pattern and the excitation beam pattern. The antenna's total quality factor ( $Q$ ) is the summation of radiation quality factor ( $Q_{\text{rad}}$ ) and absorption quality factor ( $Q_{\text{abs}}$ ):  $Q^{-1} = Q_{\text{rad}}^{-1} + Q_{\text{abs}}^{-1}$ . This equation gives an intuitive picture that the field enhancement of an optical antenna is proportional to two important factors: antenna efficiency ( $Q/Q_{\text{rad}}$ ) and Purcell enhancement factor<sup>19</sup> ( $Q/V_{\text{eff}}$ ).

Using the equation for the field enhancement, there are five parameters that can be optimized to achieve maximum field enhancement:

**Received:** February 3, 2011  
**Revised:** May 11, 2011  
**Published:** June 07, 2011

- 1 The antenna needs to be excited on resonance ( $\lambda_{\text{res}}$ ),<sup>16</sup> which can be achieved by tuning the antenna dimensions<sup>8</sup> or loading the antenna gap with appropriate materials.<sup>9,14</sup>
- 2 The effective mode volume of the antenna ( $V_{\text{eff}}$ ) needs to be reduced, which can be achieved by shrinking the size of antenna feed gap.<sup>2,20</sup>
- 3 The maximum effective aperture ( $A_c$ ) needs to be optimized through matching the antenna's radiation pattern with the excitation signal.<sup>21</sup> For example, the radiation pattern can be optimized to match plane wave excitation using an antenna array since the effective aperture is proportional to the directivity of the antenna and the directivity can be increased by the array factor.<sup>22</sup>
- 4 Another parameter that has not yet been explored and which we will discuss in this work is the optimum condition for an antenna's relevant loss rates (i.e.,  $Q$ ,  $Q_{\text{rad}}$ ,  $Q_{\text{abs}}$ ). To

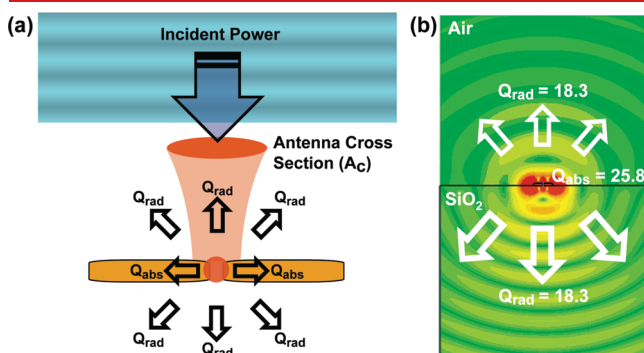


**Figure 1.** (a) Schematic and modeling of a dipole antenna as a resonator using the coupled mode theory (CMT). (b) Simulation of a dipole antenna on a quartz glass. Most of the radiation from the antenna is lost to the substrate resulting in a poor coupling from the plane wave excitation to the antenna.

find the optimum, we take the derivative of eq 1 with respect to  $Q_{\text{rad}}$  and equate it to 0 (Supporting Information, Section II). Since the effective aperture ( $A_c$ ), effective mode volume ( $V_{\text{eff}}$ ), and the  $Q_{\text{abs}}$  vary slowly compared to  $Q_{\text{rad}}$  (see Section III in Supporting Information and Figure 2c), the maximum field enhancement condition is achieved when  $Q_{\text{rad}}$  becomes equal to  $Q_{\text{abs}}$

$$Q_{\text{rad}} = Q_{\text{abs}} \quad (2)$$

This is analogous to the impedance matching concept in antenna theory.<sup>23–25</sup>

- 5 At the optimum  $Q$  condition ( $Q_{\text{rad}} = Q_{\text{abs}} = 2Q$ ), the expression for the field enhancement reduces to

$$\frac{|E_{\text{loc}}|^2}{|E_i|^2} = \frac{A_c \lambda}{\pi} \frac{Q}{V_{\text{eff}}} = \frac{A_c \lambda}{2\pi} \frac{Q_{\text{abs}}}{V_{\text{eff}}} \quad (3)$$

Therefore, the optimized field enhancement for given material is directly proportional to absorption quality factor ( $Q_{\text{abs}}$ ), which is a direct evidence of previously reported<sup>21</sup> high field enhancement with low loss material (such as silver).

From the above recipe to achieve maximum field enhancement for optical antennas, items 1, 2, 3, and 5 have previously been demonstrated. Here, we will introduce the concept of  $Q$ -matching for optical antennas (item 4) and achieve the optimum condition through radiation engineering. As the starting point, we will study the radiation characteristics of a typical optical antenna fabricated on a glass substrate. To estimate the amount of mismatch between  $Q_{\text{rad}}$  and  $Q_{\text{abs}}$  for a gold dipole antenna (with 260 nm length, 40 nm width, 25 nm thickness, and 15 nm gap) on a quartz glass substrate, we have used time domain simulations based on finite integrate technique (CST Microwave Studio) to calculate  $Q$ ,  $Q_{\text{rad}}$ , and  $Q_{\text{abs}}$ .

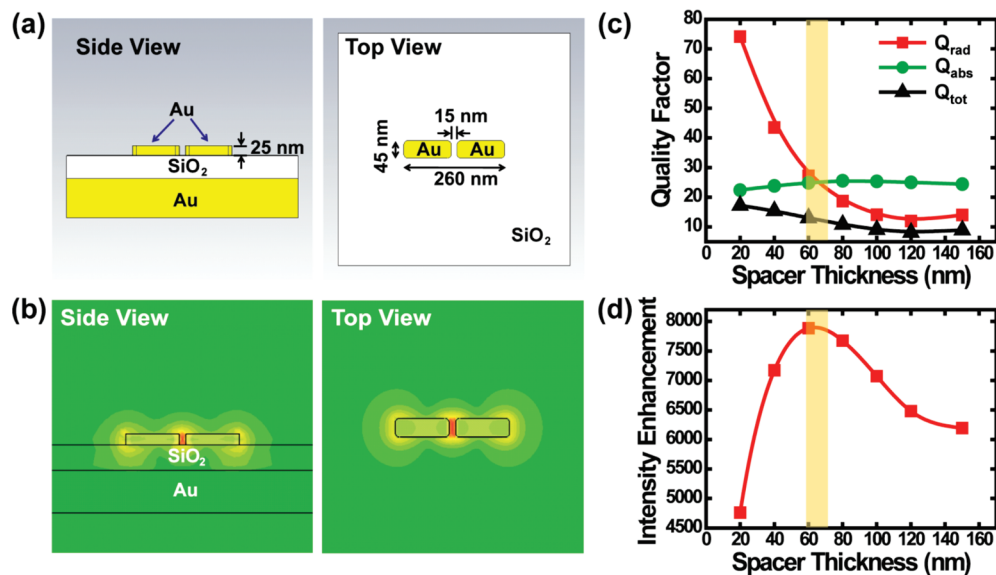


**Figure 2.** Numerical simulations of a gold optical dipole antenna array on a gold ground plane. (a) Schematic picture of simulated structure. The 260 nm long, 45 nm wide, and 25 nm thick gold dipole antennas with 15 nm gap on gold ground plane were simulated using a time domain solver based software. Periodic boundary condition was used to calculate an antenna array with 600 nm pitch. (b) Electric field magnitude distribution of simulated dipole antennas. (c) Quality factor plot as a function of  $\text{SiO}_2$  dielectric spacer thickness. (d) Field intensity enhancement plot as a function of  $\text{SiO}_2$  dielectric spacer thickness. Electric field is measured at the center of dipole antenna gap. The field intensity enhancement has a maximum peak at the optimum spacer thickness for  $Q$ -matching ( $Q_{\text{rad}} = Q_{\text{abs}}$ ) condition.

The total quality factor of the antenna ( $Q$ ) and the radiation  $Q$  of the antenna are calculated to be  $Q = 10.7$  and  $Q_{\text{rad}} = 18.3$ , respectively. The total quality factor of the antenna,  $Q_t$ , consists of the radiation ( $Q_{\text{rad}}$ ) and absorption ( $Q_{\text{abs}}$ ),  $Q_t^{-1} = Q_{\text{abs}}^{-1} + Q_{\text{rad}}^{-1}$ . Therefore, the absorption  $Q$  of the antenna can be calculated as  $Q_{\text{abs}}^{-1} = Q_t^{-1} - Q_{\text{rad}}^{-1} = 10.7^{-1} - 18.3^{-1} = 25.8^{-1}$ . This mismatch between the radiation  $Q$  and absorption  $Q$  reduces the energy coupling into optical antennas, leading to smaller field enhancements.

To improve the antenna efficiency through  $Q$  matching, we need to controllably tune either the radiation  $Q$  or absorption  $Q$  of the antenna. Since absorption  $Q$  of the antenna is dictated by the metal loss (gold or silver), the radiation  $Q$  of the antenna needs to be tuned. We achieve this radiation engineering of optical antennas using dielectric spacer coated metal ground planes (Figure 2a). Metallic ground planes have been used previously to enhance the fluorescence or SERS of molecules placed a distance of quarter-wavelength ( $\lambda/4$ ) away from the ground plane using a dielectric spacer.<sup>17,18</sup> The  $\lambda/4$  distance results in constructive interference between the top and bottom reflected emissions of the molecule and increases the effective aperture  $A_e$ . However, in addition to reflecting the bottom radiation, the ground plane can be used to control the radiation  $Q$  of the antenna and tune it to match the absorption  $Q$  of antenna. For example, as the dielectric spacer thickness is reduced beyond the quarter-wavelength ( $\lambda/4$ ) thickness, the antenna dipole and the antenna image dipole radiation cancel each other more and more. Therefore, as the dielectric spacer thickness is reduced, the radiation  $Q$  of the antenna is increased and at the optimum dielectric spacer thickness, the radiation and absorption  $Q$  of the antenna would be matched, which leads to the maximum field enhancement condition.

We have used numerical simulation to verify this idea for a gold dipole antenna array on dielectric ( $\text{SiO}_2$ ) coated gold ground plane as shown in Figure 2a. Gold dipole antenna arrays with 260 nm length, 40 nm width, 25 nm thickness, 15 nm gap, and 600 nm pitch were simulated using a finite integration technique based software (CST Microwave Studio). The dipole antenna array is excited by a plane wave from the top that is polarized along the dipole antenna's long axis. As indicated in Figure 2b, the electric field is mainly confined at the antenna feed gap on resonance. The total  $Q$ , radiation  $Q$ , and absorption  $Q$  of the antenna array are calculated as the thickness of  $\text{SiO}_2$  spacer layer is varied from 20 to 150 nm. As shown in Figure 2c, the radiation  $Q$  increases as the thickness of spacer decreases, which is expected from the radiation cancellation between the real and the image dipole antenna. The radiation  $Q$  matches with the absorption  $Q$  at the spacer layer thickness of 60 nm. The field intensity enhancement is also maximized at this optimum spacer thickness (60 nm), which agrees well with our theory (Figure 2d). It is important to note that the optimum dielectric spacer thickness (60 nm) is less than half of the quarter-wavelength thickness of 150 nm.

To experimentally verify the  $Q$ -matching condition, gold optical dipole antenna arrays were fabricated on  $\text{SiO}_2$  spacer coated gold ground planes using high resolution e-beam lithography and a lift-off process. For the ground plane, a 100 nm thick gold layer was evaporated on a Si wafer, and  $\text{SiO}_2$  layers of various thicknesses (20, 60, 100, and 150 nm) were deposited using plasma-enhanced chemical vapor deposition (PECVD). We patterned 260 nm long and 45 nm wide optical dipole antennas using e-beam lithography followed by evaporation of 3 nm thick germanium and 25 nm thick gold. Germanium adhesion layers reduce the roughness of gold surface<sup>26</sup> (Supporting Information,

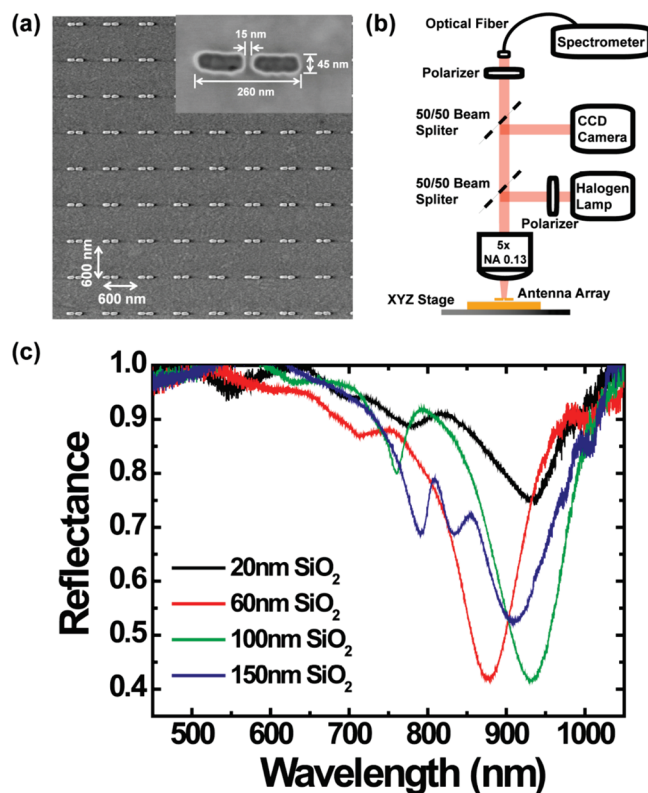


**Figure 3.** Characterization of the fabricated optical antennas. (a) SEM image of fabricated gold antenna arrays on a dielectric ( $\text{SiO}_2$ ) coated gold ground plane. The inset shows a typical dipole antenna with 260 nm length, 45 nm width, and 15 nm gap. (b) The reflection measurement setup for characterization of dipole antennas. (c) Normalized reflection (reflectance) spectra of the dipole antenna arrays for various dielectric ( $\text{SiO}_2$ ) thicknesses. The 100 nm  $\text{SiO}_2$  thickness displays the largest reflection dip, corresponding to strongest field enhancement as predicted by the theory. Reflectance spectra show two major dips for each array. The larger dip position at longer wavelength corresponds to the antenna resonance and smaller dip corresponds to surface plasmon resonance supported by the periodic array.

Section IV). The total size of the optical antenna array field is  $300 \mu\text{m} \times 300 \mu\text{m}$  and identical dipole antennas were distributed with a 600 nm pitch (square array). Figure 3a shows the SEM picture of fabricated optical dipole antenna array and the typical dimensions of a single antenna are shown in the inset. Each antenna has a length of 260 nm, width of 45 nm, and gap of 15 nm. We use reflectance measurements to characterize the optical antennas and the effect of  $Q$ -matching since this measurement method is less sensitive to variations in parameters such as gap spacing caused by nonuniformities in e-beam lithography exposure. The illumination from a halogen lamp was focused on the antenna array using a  $5\times$ ,  $\text{NA} = 0.13$  objective lens and the reflection from the antenna array was collected through the same objective lens and sent to the spectrometer using a multicore optical fiber (Figure 3b). Figure 3c shows the normalized reflection spectrum (reflectance) of the antenna arrays for various dielectric spacer thicknesses, each spectrum is calculated by dividing the reflection from the antenna arrays with the reflection from an area on the dielectric coated ground plane without any antennas. Reflectance spectra show two major dips for each array. The larger dip position at longer wavelength corresponds to the antenna resonance and smaller dip corresponds to surface plasmon resonance supported by the periodic array.

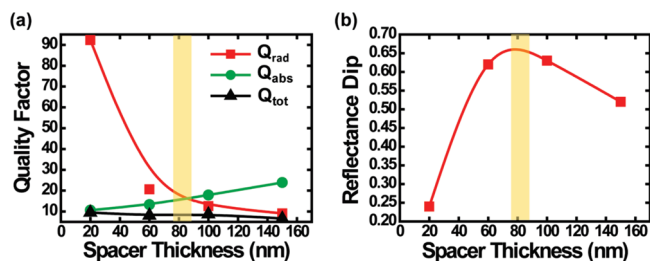


**Figure 4.** (a) Experimental values of radiation, absorption, and total quality factors as a function of the dielectric spacer thickness. The trend follows closely the simulation with the  $Q$ -matching ( $Q_{\text{rad}} = Q_{\text{abs}}$ ) condition achieved at  $\sim 80$  nm dielectric thickness. (b) Reflectance dip of optical antennas as a function of the dielectric spacer. The maximum reflectance dip, corresponding to maximum field enhancement, is achieved for the  $Q$ -matched dielectric thickness.

Various parameters such as resonance wavelength, total  $Q$ , radiation  $Q$ , and absorption  $Q$  of the antenna can be extracted from the reflectance measurements. The resonance wavelength and total  $Q$  are extracted directly by fitting a Lorentzian curve to the reflectance spectrum. Radiation  $Q$  is calculated using reflectance equation from modified CMT<sup>27</sup> (Supporting Information, Section V) to take into account the uncoupled portion of the plane wave excitation. The absorption  $Q$  of the antenna array is then calculated using the relation  $Q_{\text{abs}}^{-1} = Q^{-1} - Q_{\text{rad}}^{-1}$ . The extracted radiation  $Q$ , absorption  $Q$ , and total  $Q$  of the antenna arrays are shown in Figure 4a as a function of dielectric spacer thickness. The optimum dielectric spacer thickness at which the antenna array's radiation  $Q$  and the absorption  $Q$  are matched is approximately 80 nm. The size of dip in the reflectance measurements is proportional to the maximum field enhancement (Supporting Information, Section V), as shown in Figure 4b, the maximum dip in reflectance measurement is also achieved for a dielectric spacer close to 80 nm, which is consistent with the  $Q$ -matching condition. It is important to note that this optimum thickness ( $\sim 80$  nm) is roughly half of the quarter-wavelength thickness and results in approximately 20% larger field enhancement.

In conclusion, we introduce a new condition to achieve maximum field enhancement for optical antennas through matching the radiation  $Q$  and absorption  $Q$  of the antenna. This matching is achieved experimentally by fabricating an array of dipole antennas on a dielectric coated ground plane and tuning the thickness of the dielectric spacer to control the antennas' radiation  $Q$ . The maximum field enhancement is achieved at the optimum dielectric thickness of  $\sim 80$  nm, which results in  $Q_{\text{rad}} = Q_{\text{abs}}$ . This is slightly higher than the optimum thickness from simulation probably due to the more loss of fabricated metal, however, general trends show good agreement with theory and simulation. The optimum spacer thickness is  $\sim 50\%$  smaller than the quarter-wavelength thickness and achieves  $\sim 20\%$  larger reflectance.

## ■ ASSOCIATED CONTENT

**S** **Supporting Information.** Additional information provided. This material is available free of charge via the Internet at <http://pubs.acs.org>.

## ■ AUTHOR INFORMATION

### Corresponding Author

\*E-mail: [wu@eecs.berkeley.edu](mailto:wu@eecs.berkeley.edu).

## Author Contributions

<sup>S</sup>These authors contributed equally to this work.

## ■ ACKNOWLEDGMENT

This work was supported in part by DARPA SERS S&T Fundamentals No. FA9550-08-1-0257. Work at the Molecular Foundry was supported by the Director, Office of Science, Office of Basic Energy Sciences, Division of Materials Sciences and Engineering, of the U.S. Department of Energy under Contract No. DE-AC02-05CH11231. The authors would like to thank Professor Luke P. Lee and Professor Kyoungsik Yu. The authors declare no competing financial interests.

## ■ REFERENCES

- (1) Crozier, K. B.; Sundaramurthy, A.; Kino, G. S.; Quate, C. F. Optical antennas: Resonators for local field enhancement. *J. Appl. Phys.* **2003**, *94*, 4632.
- (2) Schuck, P. J.; Fromm, D. P.; Sundaramurthy, A.; Kino, G. S.; Moerner, W. E. Improving the Mismatch between Light and Nanoscale Objects with Gold Bowtie Nanoantennas. *Phys. Rev. Lett.* **2005**, *94*, 017402.
- (3) Schuller, J. A.; Taubner, T.; Brongersma, M. L. Optical antenna thermal emitters. *Nat. Photonics* **2009**, *3*, 658–661.
- (4) Tang, L.; et al. Nanometre-scale germanium photodetector enhanced by a near-infrared dipole antenna. *Nat. Photonics* **2008**, *2*, 226–229.
- (5) Challener, W. A.; et al. Heat-assisted magnetic recording by a near-field transducer with efficient optical energy transfer. *Nat. Photonics* **2009**, *3*, 220–224.
- (6) Nie, S.; Emory, S. R. Probing Single Molecules and Single Nanoparticles by Surface-Enhanced Raman Scattering. *Science* **1997**, *275*, 1102–1106.
- (7) Kneipp, K.; et al. Single Molecule Detection Using Surface-Enhanced Raman Scattering (SERS). *Phys. Rev. Lett.* **1997**, *78*, 1667.
- (8) Zhang, W.; Fischer, H.; Schmid, T.; Zenobi, R.; Martin, O. J. F. Mode-Selective Surface-Enhanced Raman Spectroscopy Using Nanofabricated Plasmonic Dipole Antennas. *J. Phys. Chem. C* **2009**, *113*, 14672–14675.
- (9) Alù, A.; Engheta, N. Input Impedance, Nanocircuit Loading, and Radiation Tuning of Optical Nanoantennas. *Phys. Rev. Lett.* **2008**, *101*, 043901.
- (10) Huang, J.-S.; Feichtner, T.; Biagioni, P.; Hecht, B. Impedance Matching and Emission Properties of Nanoantennas in an Optical Nanocircuit. *Nano Lett.* **2009**, *9*, 1897–1902.
- (11) Chu, Y.; Crozier, K. B. Experimental study of the interaction between localized and propagating surface plasmons. *Opt. Lett.* **2009**, *34*, 244–246.
- (12) Haus, H. *Waves and fields in optoelectronics*; Prentice-Hall: Englewood Cliffs NJ, 1984.
- (13) Maier, S. A. Plasmonic field enhancement and SERS in the effective mode volume picture. *Opt. Express* **2006**, *14*, 1957–1964.
- (14) Alu, A.; Engheta, N. Tuning the scattering response of optical nanoantennas with nanocircuit loads. *Nat Photonics* **2008**, *2*, 307–310.
- (15) Merlein, J.; et al. Nanomechanical control of an optical antenna. *Nat. Photonics* **2008**, *2*, 230–233.
- (16) Novotny, L. Effective Wavelength Scaling for Optical Antennas. *Phys. Rev. Lett.* **2007**, *98*, 266802.
- (17) Ray, K.; Mason, M. D.; Yang, C.; Li, Z.; Grober, R. D. Single-molecule signal enhancement using a high-impedance ground plane substrate. *Appl. Phys. Lett.* **2004**, *85*, 5520.
- (18) Min, Q.; et al. Substrate-based platform for boosting the surface-enhanced Raman of plasmonic nanoparticles. *Opt. Express* **2011**, *19*, 1648–1655.
- (19) Purcell, E. Spontaneous emission probabilities at radio frequencies. *Phys. Rev.* **1946**, *69*, 681.

(20) Lim, D.-K.; Jeon, K.-S.; Kim, H. M.; Nam, J.-M.; Suh, Y. D. Nanogap-engineerable Raman-active nanodumbbells for single-molecule detection. *Nat. Mater.* **2010**, *9*, 60–67.

(21) Chu, Y.; Banaee, M. G.; Crozier, K. B. Double-Resonance Plasmon Substrates for Surface-Enhanced Raman Scattering with Enhancement at Excitation and Stokes Frequencies. *ACS Nano* **2010**, *4*, 2804–2810.

(22) Stutzman, W. L.; Thiele, G. A. *Antenna Theory and Design*, 2nd ed.; Wiley: New York, 1997.

(23) Kwon, D.-H.; Pozar, D. M. Optimal Characteristics of an Arbitrary Receive Antenna. *IEEE Trans. Antennas Propag.* **2009**, *57*, 3720–3727.

(24) Collin, R. E. Limitations of the Thevenin and Norton equivalent circuits for a receiving antenna. *IEEE Trans. Antennas Propag.* **2003**, *45*, 119–124.

(25) Alu, A.; Maslovski, S. Power Relations and a Consistent Analytical Model for Receiving Wire Antennas. *IEEE Trans. Antennas Propag.* **2010**, *58*, 1436–1448.

(26) Logeeswaran, V. J.; et al. Ultrasmooth Silver Thin Films Deposited with a Germanium Nucleation Layer. *Nano Lett.* **2009**, *9*, 178–182.

(27) Hamam, R. E.; Karalis, A.; Joannopoulos, J. D.; Soljacaroni-cacute, M. Coupled-mode theory for general free-space resonant scattering of waves. *Phys. Rev. A* **2007**, *75*, 053801.